THE ASTROPHYSICAL JOURNAL, 486:L11–L14, 1997 September 1

THE EVOLUTION OF THE GLOBAL STAR FORMATION HISTORY AS MEASURED FROM THE HUBBLE DEEP FIELD[1]

A. J. CONNOLLY, A. S. SZALAY, MARK DICKINSON,[2,3] M. U. SUBBARAO, AND R. J. BRUNNER
Department of Physics and Astronomy, Johns Hopkins University, Baltimore, MD 21218; ajc@skysrv.pha.jhu.edu, szalay@skysrv.pha.jhu.edu, med@stsci.edu, subbarao@skysrv.pha.jhu.edu, rbrunner@skysrv.pha.jhu.edu
Received 1997 April 8; accepted 1997 June 13

ABSTRACT

The Hubble Deep Field (HDF) is the deepest set of multicolor optical photometric observations ever undertaken, and it offers a valuable data set with which to study galaxy evolution. Combining the optical WFPC2 data with ground-based near-infrared photometry, we derive photometrically estimated redshifts for HDF galaxies with $J < 23.5$. We demonstrate that incorporating the near-infrared data reduces the uncertainty in the estimated redshifts by approximately 40% and is required to remove systematic uncertainties within the redshift range $1 < z < 2$. Utilizing these photometric redshifts, we determine the evolution of the comoving ultraviolet (2800 Å) luminosity density (presumed to be proportional to the global star formation rate) from a redshift of $z = 0.5$ to $z = 2$. We find that the global star formation rate increases rapidly with redshift, rising by a factor of 12 from a redshift of zero to a peak at $z \approx 1.5$. For redshifts beyond 1.5, it decreases monotonically. Our measures of the star formation rate are consistent with those found by Lilly et al. from the Canada-France Redshift Survey at $z < 1$ and by Madau et al. from Lyman break galaxies at $z > 2$, and they bridge the redshift gap between those two samples. The overall star formation or metal enrichment rate history is consistent with the theoretical models of White and Frenk and the predictions of Pei and Fall based on the evolving H I content of Lyα QSO absorption line systems.

Subject headings: galaxies: evolution — galaxies: fundamental parameters — techniques: photometric

1. INTRODUCTION

The multicolor photometric survey of the Hubble Deep Field (HDF; Williams et al. 1996) provides a unique opportunity for studying the evolution of the global star formation history of the universe. Quantifying this relation has significant consequences for the evolution of structure formation, supernova rates, and the metal enrichment of the intergalactic medium as a function of epoch. For redshifts less than one, the Canada-France Redshift Survey (CFRS; Lilly et al. 1996) has shown that the comoving UV (2800 Å) luminosity density of galaxies increases rapidly as a function of redshift, rising by a factor of about 15 from $z = 0$ to 1. Because the UV luminosity of star-forming galaxies is, broadly speaking, proportional to their star formation rates (SFRs), this change in luminosity density has been inferred to trace a global decline in the cosmic SFR since $z = 1$. Using the 1500 Å luminosity of galaxies in the HDF selected by the presence of a Lyman continuum break, Madau et al. (1996) find that the inferred SFR at $z > 2$ is lower than the value measured by the CFRS at $z \approx 1$ and falls steadily toward higher redshifts. The implication of these two surveys is that the comoving luminosity density peaks somewhere within the redshift range $1 < z < 2$. To date, however, there have been no systematic surveys of this redshift range; consequently, the evolution of the luminosity density for $1 < z < 2$ remains a matter of conjecture. Based on the evolution of the global H I content of the universe as measured from Lyα QSO absorption line systems, Pei & Fall (1995) have predicted that the cosmic SFR should peak somewhere in this redshift range. It therefore seems worthwhile to undertake a study of the global SFR within this redshift regime. Throughout this letter we assume an $\Omega = 1$, $q_0 = 0.5$ cosmology.

2. NEAR-INFRARED OBSERVATIONS OF THE HUBBLE DEEP FIELD

To complement the optical multicolor data of the HDF, follow-up near-infrared observations were undertaken with the KPNO 4 m telescope. Full details of the observations and data reduction will be described in Dickinson et al. (1997); we briefly summarize the salient features here.

At the f/15 focus of the Mayall 4 m telescope, the infrared imager (IRIM) 256×256 Rockwell NICMOS-3 HgCdTe infrared array covers a 2.′56 field of view with a 0.′6 pixel scale. The field of view of IRIM is, therefore, well matched to the WFPC2 images. Over the course of 10 days, a total of 11.0, 11.3, and 22.9 hr of data were collected for the HDF in the J, H, and K_s passbands. The formal magnitude limits for a 2″ aperture and a signal-to-noise ratio of 5 are 23.45, 22.29, and 21.92 in the J, H, and K_s filters, respectively.

All images were combined using a "drizzling" method similar to that applied to the optical HDF data (Fruchter & Hook 1997). This resulted in a plate scale of 0.″1594 pixel^{-1}. The near-infrared images were registered and transformed to the same geometry as the optical WFPC2 frames (after binning down the optical images to the pixel scale of the near-infrared data).

[1] Based on observations made with the NASA/ESA *Hubble Space Telescope*, obtained from the data archive at the Space Telescope Science Institute, which is operated by the Association of Universities for Research in Astronomy, Inc., under cooperative agreement with the National Science Foundation.

[2] Visiting observer at the Kitt Peak National Observatory, National Optical Astronomy Observatories, which is operated by the Association of Universities for Research in Astronomy, Inc. (AURA) under cooperative agreement with the National Science Foundation.

[3] Space Telescope Science Institute.

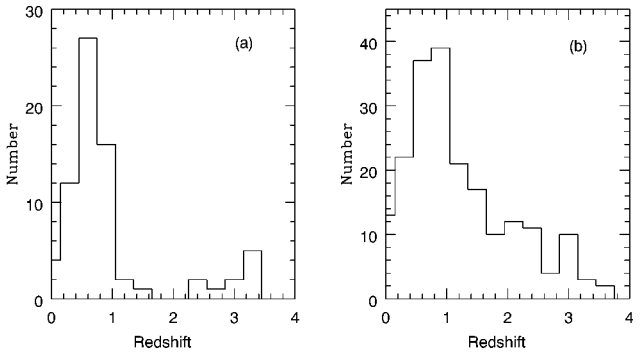

FIG. 1.—The redshift distribution for those galaxies within the HDF with $J < 23.5$. (*a*) Distribution for those galaxies with measured spectroscopic redshifts; (*b*) derived redshift distribution for the photometric redshift sample. The peak in the $n(z)$, at $z \sim 0.9$, for our photometric redshift sample is in reasonable agreement with that predicted from gravitational lensing (Ebbels et al. 1997).

3. OPTICAL AND NEAR-INFRARED PHOTOMETRIC CATALOGS

For the purposes of this Letter, we wish to select galaxies from the HDF in a fashion similar to that used for the CFRS survey, which has been used to estimate the redshift evolution of global SFRs at $z < 1$. The CFRS galaxy sample was derived from *I*-band photometry so as to select objects on the basis of their rest frame optical ($\lambda_0 > 4000$ Å) emission out to $z \approx 1$. In order to reproduce broadly this strategy at higher redshift, we have chosen our HDF galaxy sample in the *J*-band (i.e., at $\lambda_{obs} \approx 12500$ Å). This ensures that in the $1 < z < 2$ redshift range of interest here, galaxies are selected at similar rest frame wavelengths as the *I*-band CFRS probes for $0.2 < z < 1$. The *J* band is approximately equivalent to a redshifted rest frame *B* band at $z = 1.9$.

Photometric catalogs for the optical and near-infrared data were constructed using a modified version of the SExtractor image analysis program (Bertin & Arnouts 1996). Object detection was carried out using a 1″ FWHM Gaussian detection kernel on the *J* image. Matched aperture photometry was performed on each of the optical and near-infrared images. A 4″ diameter aperture was placed on each object detected in the *J*-band data. To reduce the effect of flux from nearby objects contaminating these aperture magnitudes, SExtractor was modified to mask out nearby sources (Brunner 1997).

The resulting optical and near-infrared catalog contains a total of 219 galaxies to a magnitude limit of $J < 23.5$. At $z = 2$ for our adopted cosmology, this *J*-band apparent magnitude limit corresponds to a rest frame absolute magnitude of $B = -20.4$, or approximately 0.6 mag fainter than present-day L^* (i.e., assuming no luminosity evolution). Of the cataloged sources, 194 and 204 were detected independently in the *H* and K_s passbands. At these signal-to-noise levels, all objects in our infrared catalog have optical counterparts in the WFPC2 images. Of these, 73 have measured spectroscopic redshifts (Cohen et al. 1996; Steidel et al. 1996b; Lowenthal et al. 1997). Their redshift distribution is shown in Figure 1*a*.

4. AN EMPIRICAL APPROACH TO PHOTOMETRIC REDSHIFTS

A number of attempts have been made to estimate the redshifts and spectral types of galaxies from broadband photometry using ground-based data (Koo 1985; Connolly et al. 1995). The success of these studies led to the application of photometric redshifts to optical data for the HDF (Gwyn & Hartwick 1996; Mobasher et al. 1996; Lanzetta, Yahil, & Fernández-Soto 1996; Sawicki, Lin, & Yee 1996). In the above references, a comparison between the spectroscopic and photometric redshifts has been shown to result in a dispersion of $\sigma_z \sim 0.15$ in the redshift ranges $0 < z < 1$ and $2.2 < z < 3.5$. However, there are significantly larger errors in the $1 < z < 2$ regime.

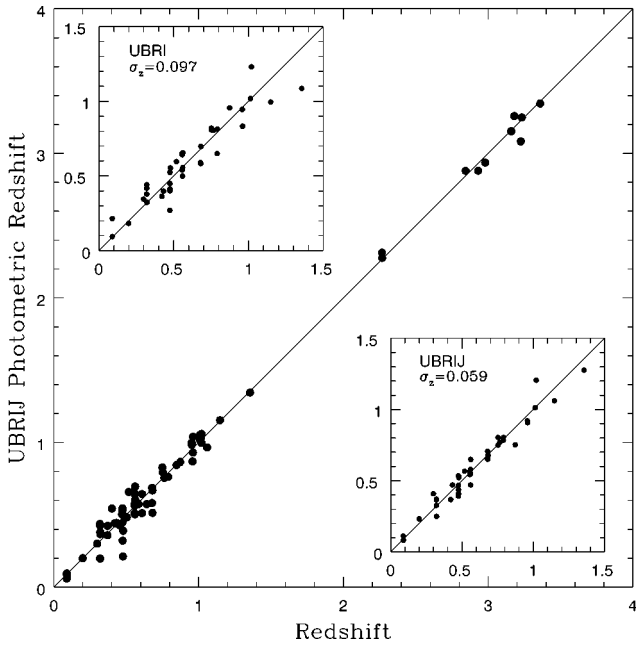

FIG. 2.—A comparison between the spectroscopic and photometric redshifts for the HDF sample. The inset panels show the effect of including the near-infrared data into the photometric redshift relation. The top inset shows the derived relation for the F300W, F450W, F606W, and F814W passbands (for galaxies with $z < 1.5$). The dispersion in the relation is $\sigma_z = 0.097$. The lower inset shows the dispersion for the F300W, F450W, F606W, F814W, and *J* passbands. The dispersion decreases to $\sigma_z = 0.059$. The correlation for all galaxies within the HDF ($J < 23.5$) is given in the main figure.

The increase in the dispersion for $z > 1$ is due to the HDF passbands sampling the optical and near-UV rest frame wavelengths. The dominant feature that provides the photometric redshift is the transition of the break in the galaxy continuum around 4000 Å through the F450W and F606W filters (Connolly et al. 1995). At $z > 1$ this break moves out of the optical spectral region and into the near-infrared. For star-forming galaxies, the UV continuum from Lyα (1215 Å) to about 3000 Å is relatively devoid of strong features; consequently, there is little information in optical photometry from which to estimate redshifts at $1 < z < 2$. At redshifts greater than 2.2, the 912 Å Lyman limit enters the *U* band, and redshifts can again be estimated in an analogous manner to the 4000 Å discontinuity (Steidel et al. 1996a, 1996b; Madau et al. 1996).

Therefore, using only the HDF optical data, the redshift range from $1 < z < 2$ is poorly constrained. With the addition of deep *J*-band data alone, we can detect the transition of the 4000 Å discontinuity out to $z = 2.1$. To demonstrate this, in Figure 2 we fit a quadratic relation between the HDF optical magnitudes (only) and the spectroscopic redshifts (for galaxies with $z < 1.5$). The dispersion about this relation is $\sigma_z = 0.097$. The dispersion increases as a function of redshift, doubling by a redshift of one. If we incorporate the near-infrared *J*-band data and refit the relation, the dispersion decreases by 40% ($\sigma_z = 0.059$). Similar success has been

TABLE 1

COMOVING 2800 Å LUMINOSITY DENSITY

			LUMINOSITY FUNCTION CORRECTED[a]		
REDSHIFT (1)	OBSERVED[a] (2)	M^* (3)	$\alpha = -1.0$ (4)	$\alpha = -1.3$ (5)	$\alpha = -1.5$ (6)
0.5–1.0	19.30	−20.25	19.43	19.52	19.65
1.0–1.5	19.48	−21.00	19.55	19.69	19.85
1.5–2.0	19.38	−21.75	19.39	19.59	19.62

[a] $\log L$ (2800 Å) in h_{50}^{-2} W Hz^{-1} Mpc^{-3}.

reported by Cowie (1996; see also Ellis 1997) using an independent infrared data set and a different redshift estimation methodology.

To derive the estimated photometric redshifts out to $z = 2$, we fit a third-order polynomial in the F300W, F450W, F606W, F814W and J passbands to the observed spectroscopic data (full details of our technique can be found in Connolly et al. 1995 and Brunner et al. 1997). The correlation between the spectroscopic and photometric redshifts is given in Figure 2. The dispersion within this relation is $\sigma_z = 0.06$. Applying this relation to those galaxies without spectroscopic redshifts, we derive the photometric redshift sample. In Figure 1*b* we show a comparison between the observed redshift distribution for the spectroscopic data and the redshift distribution determined from the third-order fit to the optical and near-infrared data.

One advantage of our technique is that it does not depend on the assumption of any particular set of template spectral energy distributions for the galaxies (see Ellis 1997). The corresponding limitation to the method is that it requires a calibrating sample of galaxies with spectroscopic redshifts. In the redshift interval $1 < z < 2$ there are currently only a handful of galaxies with spectroscopic redshifts. We therefore utilize those galaxies with $z > 2$ to constrain the high-redshift portion of the photometric redshift relation; we do not use them in our subsequent analysis of the evolution of the comoving luminosity density.

5. EVOLUTION OF THE GLOBAL STAR FORMATION RATE

The evolution of the comoving UV luminosity density has been characterized by Lilly et al. (1996) for the redshift interval $0 < z < 1$, and by Madau et al. (1996) for $z > 2$. Lilly et al. (1996) derived 2800 Å luminosity densities for the CFRS galaxy sample, while Madau et al. (1996) used 1500 Å luminosities for Lyman break galaxies in the HDF. Madau et al. (1996) employ spectral population synthesis models to compute conversions from luminosity at these two UV wavelengths to SFRs and metal enrichment rates (MERs), permitting comparison of these quantities for galaxy samples at widely varying redshifts. The conversion to MER is less sensitive to the assumed form of the initial mass function than is the conversion to SFR.

Using the photometric redshift sample, we investigate the redshift dependence of the SFR in the range $0.5 < z < 2$. This lower redshift limit ensures that the HDF optical passbands always sample rest frame wavelengths $\lambda > 2000$ Å. Galaxy luminosities at 2800 Å can therefore be interpolated directly from the observed multicolor photometry. This allows us to compare our results directly with those of Lilly et al. (1996). The upper redshift limit is imposed because at redshift $z > 2$ the break in the galaxy spectral energy distribution at 4000 Å moves out of the J band (see § 4 above).

We construct the comoving luminosity density for three redshift ranges: $0.5 < z < 1$, $1 < z < 1.5$ and $1.5 < z < 2$. The observed luminosity densities in these redshift intervals are given in column (2) of Table 1. Because our sample is limited to galaxies with $J < 23.5$, it samples different luminosity ranges at each redshift. Following the procedure of Lilly et al. (1996), we correct for the incompleteness in the observed luminosity densities by integrating over a Schechter luminosity function for each redshift bin. Column (3) of Table 1 gives the value of M^* (at 2800 Å, in AB magnitudes) derived from the photometric data for each of the redshift intervals. Columns (4), (5), and (6) give the corrected comoving luminosity density assuming a Schechter luminosity function with a slope of $\alpha = -1.0$, -1.3, and -1.5, respectively. For the highest redshift bin and the steepest value of α, our completeness correction is approximately a factor of 2.

With our current data set we cannot reliably determine the evolution of the faint-end slope of the luminosity function with redshift. For comparison with the CFRS sample, we assume a value of $\alpha = -1.3$ for the slope of the Schechter function (Lilly et al. 1996). The uncertainties in the derived values are estimated by considering the magnitude of the incompleteness corrections for a range in α of $-1.0 < \alpha < -1.5$. For each redshift interval these corrections give an uncertainty of approximately 0.15 in the log. We therefore adopt this value for each of the three redshift intervals.

The derived 2800 Å luminosity densities were converted to MERs to compare with the predictions of Pei & Fall (1995) and with the $z > 2$ data of Madau et al. (1996) (which, as noted, are based on 1500 Å luminosity densities). We derive this conversion using the Bruzual & Charlot (1996) stellar population synthesis models, assuming a Salpeter initial mass function, constant SFR, solar metallicity, and a galaxy age of 0.1–1 Gyr (Dickinson et al. 1997; Madau et al. 1996). The conversion from L(2800 Å) to MER is $2.2 \times 10^{-23} M_\odot$ yr^{-1} W^{-1} Hz. Note that this differs from the value adopted by Madau et al. (1996) by a factor of approximately 1.6, because of, in part, changes in the stellar synthesis models of Bruzual & Charlot (1996). The conversion from 1500 Å luminosity to MER (which is used for the $z > 2$ data points for the Lyman break galaxies) remains unchanged from the values used by Madau et al. (1996). These changes in the conversion factors go in the sense of reducing the MERs or SFRs at $0 < z < 2$ relative to those at $z > 2$.

The MER as a function of redshift from Gallego et al. (1995; *open triangle*), Lilly et al. (1996; *open circles*), and Madau (1996; *open squares*) and our photometric redshift sample (*solid circles*) is given in Figure 3. Superposed on these plots are the predictions of Pei & Fall (1995) based on the evolution of the H I content in damped Lyα systems. The solid line represents models with a comoving gas density, $\Omega_{ginf} = 4 \times 10^{-3}\ h^{-1}$, and the dashed lines those with $\Omega_{ginf} = 2 \times 10^{-3}\ h^{-1}$. Models assuming a closed box or outflow model are

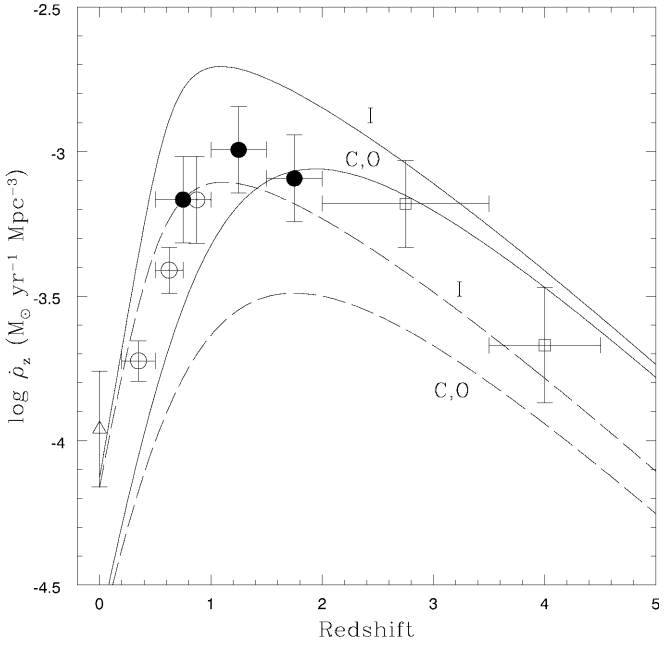

FIG. 3.—The MER as a function of redshift as measured from (*open triangle*) Gallego et al. (1995), (*open circle*) Lilly et al. (1996), and (*open square*) Madau (1996), and the photometric redshift sample (*filled circle*). The photometric redshift luminosity densities have been corrected for incompletion assuming a Schechter luminosity function with a slope of $\alpha = -1.3$. The solid and dashed lines represent the predictions of Pei & Fall (1995) for the MER based on the comoving H I density traced by Lyα absorption systems. See the text for details on the individual models.

indicated by C and O, and those assuming an inflow model by I.

6. DISCUSSION AND CONCLUSIONS

The spectroscopic, photometric, and Lyman break galaxy samples provide a remarkably consistent picture of the evolution of the MER as a function of redshift. Considering these data as a whole, we find that the comoving luminosity density rises rapidly as we look back in cosmic time from a redshift of zero to a peak at approximately $z = 1.5$. It then falls by a factor 2 out to a redshift of 3.

The amplitude and shape of the observed MER evolution with redshift are broadly consistent with the theoretical predictions of White & Frank (1991) and with the models of Pei & Fall (1995). The models with normalizations $\Omega_{\rm ginf} = 4 \times 10^{-3}\,h^{-1}$ and $\Omega_{\rm ginf} = 2 \times 10^{-3}\,h^{-1}$ bound the data points. Given the errors in the observed quantities (and in the conversions from luminosity density to MER), it is not currently feasible to try to quantify whether the data best fit a closed, open, or infall model.

The interpretation of our results depends on the absence of systematic errors in the photometric redshift technique, and on understanding the conversion of UV luminosity to MER or SFR. The close agreement between our photometric and spectroscopic redshifts (Fig. 2) encourages us to believe that the redshift estimates are good. The relative conversions between MER or SFR and luminosities at 1500 Å (for $z > 2$), 2800 Å (at $0.2 < z < 2$), and Hα ($z = 0$, from Gallego et al. 1995) depend somewhat on the assumptions of the population synthesis models. A potentially more serious effect is that of dust extinction, which may differ substantially at the various wavelengths considered here. The role of extinction in high-redshift galaxies has yet to be comprehensively analyzed from existing data sets. While extinction may be expected to have greater impact on the measurements at 1500 Å, and hence on the $z > 2$ galaxies, one must also consider the redshift evolution of the dust content of galaxies. We do not attempt to disentangle this problem here, but we call attention to it as a caution to be kept in mind.

Regardless of the absolute conversion factors, it is important to note that the comoving MERs that we calculate for the photometric redshift sample are derived in the same manner as was done for the CFRS, using luminosity densities at 2800 Å, providing a *relatively* consistent methodology across the very large redshift range $0.2 < z < 2$. It is encouraging that in the overlap region between the spectroscopic and photometric redshift sample the luminosity densities are comparable. Moreover, there is no evidence for a gross mismatch at the $z = 2$ transition between our data set and the Madau et al. (1996). Lyman break galaxy sample. We therefore believe that the general form of the MER evolution over a very broad cosmic time span is reliably described by these observations, which, for the first time, span the peak era in star-forming activity in the universe.

We thank Mike Fall, Yichuan Pei, and Piero Madau for many useful discussions on the interpretation of the MER and comoving luminosity density relation, and Stephane Charlot for providing the newer population synthesis models. We particularly thank the other investigators involved in the planning, observations, and data reduction of the near-infrared imaging data, especially Matt Bershady, Peter Eisenhardt, Richard Elston, and Adam Stanford. We acknowledge partial support from NASA grants AR-06394.01-95A and AR-06337.11-94A (A. J. C.), AR-06337.16-94A (M. D.), and an LTSA grant (A. S. Sz.).

REFERENCES

Bertin, E., & Arnouts, S. 1996, A&A, 117, 393
Brunner, R. J. 1997, Ph.D. thesis, Johns Hopkins Univ.
Brunner, R. J., Connolly, A. J., Szalay, A. S., & Bershady, M. A. 1997, ApJ, 482, L21
Bruzual, G., & Charlot, S. 1996, private communication
Cohen, J. G., Cowie, L. L., Hogg, D. W., Songaila, A., Blandford, R., Hu, E. M., & Shopbell, P. 1996, ApJ, 471, L5
Connolly, A. J.,Csabai, I., Szalay, A. S., Koo, D. C., Kron, R. C., & Munn, J. A. 1995, AJ, 110, 2655
Cowie, L. L. 1996, Proc. 37th Herstmonceux Conf., *HST* and the High-Redshift Universe, in press
Dickinson, M., et al. 1997, in preparation
Ebbels, T., Ellis, R. S., Kneib, J., Le Borgne, J., Pello, R., Smail, R., & Sanahuja B. 1997, MNRAS, submitted
Ellis, R. S. 1997, ARA&A, in press
Fruchter, A. S., & Hook, R. N. 1997, Linear Reconstruction of Hubble Deep Field, available at http://www.stsci.edu/fruchter/dither/drizzle.html
Gallego, J., Zamorano, J., Aragon-Salamanca, A., & Rego, M. 1995, ApJ, 455, L1
Gwyn, S. D. J., & Hartwick, F. D. A. 1996, ApJ, 468, L77
Koo, D. C. 1985, AJ, 90, 418
Lanzetta, K. M., Yahil, A., & Fernández-Soto, A. 1996, Nature, 381, 759
Lilly, S. J., Le Fevre, O., Hammer, F., & Crampton, D. 1996, ApJ 460, L1
Lowenthal, J. D., et al. 1997, ApJ, 481, 673
Madau, P. 1996, 7th Annual October Astrophysics Conf. in Maryland, Star Formation Near and Far, in press
Madau, P., Ferguson, H. C., Dickinson, M. E., Giavalisco, M., Steidel, C. C., & Fruchter, A. 1996, MNRAS, 283, 1388
Mobasher, B., Rowan-Robinson, M., Georgakakis, A., & Eaton, N. 1996, MNRAS, 282, L7
Pei, Y. C., & Fall, S. M. 1995, ApJ, 454, 69
Sawicki, M. J., Lin, H., & Yee, H. K. C. 1996, AJ, 117, 1
Steidel, C. C., Giavalisco, M., Dickinson, M., & Adelberger, K. L. 1996a, ApJ, 462, 17
———. 1996b, AJ, 112, 352
White, S. D. M., & Frenk, C. S. 1991, ApJ, 379, 52
Williams, R. E., et al. 1996, AJ, 112, 1335